HSOA Journal of Laser Research & Applications

Research Article

Multiple Material Domains Based Modal Parameter Analysis of Photonic Crystal Fiber

Paul D and Biswas R*

[1]*Applied Optics and Photonics Laboratory, Department of Physics, Tezpur University, Assam, India*

Abstract

We present here a complete modal parameter study of Photonic Crystal Fibers (PCF) entailing two different material compositions of distinct refractive indices. Incorporating second and third telecom window, the modal parameters have been analyzed utilizing Effective Index Method (EIM). Taking structural parameters such as pitch (Λ), effective core radius (R_{eff}) and diameter (d) as variable, we have estimated the modal parameters corresponding to phosphate and crown based PCF. The results of these two material based approaches have been compared and analyzed based on aforementioned geometrical parameters (Λ, R_{eff} and d). Here in, the lowest value of V parameter is found to be 1.3 and 0.22 at λ of 1.23μm for phosphate and crown based PCF which is below the cut-off range that can be utilizable in long term communication. Moreover, the dispersion value of phosphate and crown PCF is found to be ~ -0.55 x 10^{-9} and -2.4 x 10^{-9} ps/nm-km at λ of 1.23μm. These estimates have so far revealed superiority of crown PCF over phosphate. It has been observed that crown PCF possesses better tunability as compared to phosphate PCF. The reported results can be of many interests to optical engineers such as designing low loss waveguides, large mode area PCFs etc.

Key words: Effective index method; Fiber optics and optical communications; Microstructured fibers

***Corresponding author:** Rajib Biswas, Applied Optics and Photonics Laboratory, Tezpur University, Tezpur-784028, Assam, India, Tel: 03712-275564; E-mail: rajib@tezu.ernet.in

Citation: Paul D, Biswas R (2018) Multiple Material Domains Based Modal Parameter Analysis of Photonic Crystal Fiber. J Laser Res Appl 1: 002.

Received: November 23, 2017; **Accepted:** January 10, 2018; **Published:** January 25, 2018

Introduction

In recent times, Photonic Crystal Fiber (PCF) has grabbed attention of many researchers' in the field of optical communications as well as in sensing applications owing to their tunable configurations [1]. PCF comprises of wave-guiding core and cladding with periodic array of innumerable air holes. These air holes are generally characterized by special lattice structures with diameter (d) and specific air hole to air hole spacing (pitch: Λ) [1-4]. Owing to their flexible design, tunability in parameters, endless single-mode operation and several other unique properties, they are now being implemented in multitude of schemes [5]. Unlike conventional optical fiber, PCF obeys two types of guiding mechanism, namely., (a) modified total internal reflection (index guiding) and (b) Photonic Band-Gap (PBG) effect [4-5]. The former generally indulges traditional Total Internal Reflection (TIL) in which the central core is produced by solid defect in the central region being surrounded by numerous air holes in regular triangular lattice [6]. In the later, light guiding relies on coherent backscattering of light into the core [7]. Plentiful literatures deal with several well-known techniques, entailing fairly accurate study of PCF, such as Plane Wave Expansion method (PWE), Beam Propagation Method (BPM), Finite Difference Time Domain method (FDTD), finite element method (FEM) and Effective Index Method (EIM) [1-4,8]. Among them, EIM approach renders effortless computations of effective cladding index with specified effective core radii (R_{eff}) consuming least amount of time. Given to these merits of EIM, there is a special need to tailor PCFs with structural parameters in different material domains which will prove beneficial to optical designers for practical implementation. Accordingly, we have carried out a detailed study of modal parameters by adopting EIM with variable effective core radii (R_{eff}), diameter (d) and pitch (Λ) in context of different material composites, encompassing second and third communication band (O to L band). As the second and third telecom window is known to be the active window for communication purposes due to possession of low losses, we have chosen this range. It is mention worthy that a new class of PCF in the context of two dissimilar materials (viz. crown and phosphate) has been reported earlier in Paul, et al., [9,10]. In our earlier study, the modal properties of PCF have been demonstrated by keeping constant Λ and R_{eff} with respect to phosphate and crown glass materials. In this work, we have extended by utilizing variable geometrical parameters such as d, Λ, d/Λ and λ/Λ and with effective core radii (R_{eff}) of Λ [11,12] Λ/√3 [13], Λ/2 [14] and 2Λ-d [15] in second and third communication band (O to L). With reference to the structural parameters, modal parameters have been studied, analyzed and compared with the proposed material based PCFs. The aim of this study is to investigate the diminution of losses during long-term communication which will help the experimentalist in finding better candidate for practical applications. Additionally, we endeavor to investigate the variation of modal parameters related to PCF within the proposed wavelength range as well as with variable structural parameters (Λ and R_{eff}). Towards this accomplishment, we assess modal parameters are such as V parameter [16], Mode Filed Diameter (MFD) [17-19], effective mode area (A_{eff}) [20-22], beam divergence

(θ) [9,10] and dispersion [23-24], respectively. Each parameter has been studied by changing ʌ and R_{eff} for second and third communication bands in the context of phosphate and crown based PCF.

Mathematical formulation:

To study the modal property of photonic crystal fiber V parameter is considered to be one of the significant parameter. Further, the additional modal parameters such as Mode Field Diameter (MFD), beam divergence (θ) and effective area (A_{eff}) are associated to V-parameter [9,10]. Thus, alteration of V-parameter leads to alter the corresponding modal parameters. V-parameter that has been utilized in here is given by:

$$V = \frac{2\pi}{\lambda} R_{eff} \sqrt{(n_{gl} + \Delta n_d)^2 - (n_{gl} - \Delta n_{gc})^2} \qquad (1)$$

In equation (1), n_{gl} is refractive index of cladding which is considered to be glass index that is linked to core index and Δn_d (difference parameter) which is given by $\Delta n_d = n_{co} - n_{gl}$ and $\Delta n_{gc} = n_{gl} - n_{cl}$ (function of two dimensionless parameters-d/ʌ, λ/ʌ). Also, the air hole spacing i.e., pitch, ʌ=2.3 μm and radius of core R_{eff} is ʌ for proposed PCF structure (Figure 1). The additional modal parameters are given by:

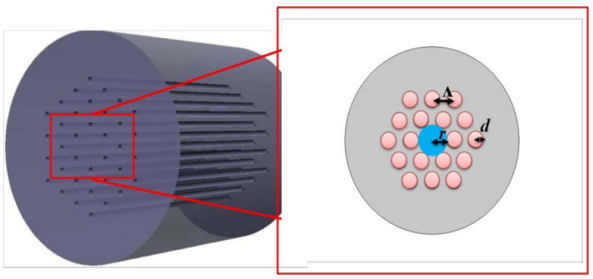

Figure 1: Schematic of the proposed structure.

Mode field diameter: $MFD = 2w_{eff}$ (2)

In which, w_{eff} is the spot size $\left(w_{eff} = R \times (0.65 + \frac{1.619}{V^{3/2}} + \frac{2.879}{V^6})\right)$ of the proposed structure

Beam divergence $\theta = \tan^{-1}(\frac{\lambda}{\pi w_{eff}})$ (3)

Effective area: $A_{eff} = k_n \pi w^2_{eff}$ (4)

In which, k_n [9, 10] is a constant.

Dispersion: $D(\lambda) = -\frac{\lambda}{c}\frac{d^2 n_{eff}}{c\lambda^2}$ (5)

Since the cladding structure of these PCFs consists of air holes, the effective index n_{eff} of the cladding shows strong wavelength dependence and is given by:

$\bar{n} = f n_{air} + (1-f) n_m$ Here n_m is the refractive index of the material of which PCF is made and λ is wavelength of propagation. Also, the air-filling factor fraction is given by $f = \frac{\pi}{2\sqrt{3}}(d/\Lambda)^2$, where d is the air-hole diameter and Λ is the pitch.

It is to be mentioned that below a certain cut-off region of V parameter, the beam is considered to be more focused towards the core as it falls under single mode region. Below the multimode region i.e., V < 2.45, the beam will be more confined and hence well guided and leading to decrease in loss. Thus, this particular parameter is a vital parameter to control during communication. Additionally, the mode radius determines the intensity of the propagated beam that has dropped down to 1/e2 of the intensity on beam axis which is associated with MFD (which is twice that of the mode radius). The effective area (A_{eff}) determines the energy in the electric field distribution of the fundamental mode. This gives the approachable effect towards the nonlinearity to the fiber optic system. This parameter also gives an estimate the area covered by the transverse dimension. Further, beam divergence confers expansion of beam from the beam waist, which is considered to be one of the vital parameter to control during communication. During the work, these aforementioned parameters has been evaluated with contribution of variable material composition as well as the geometrical parameters (ʌ, R_{eff} and d).

Adopting computationally efficient EIM technique, we have made an extensive study of the modal parameters of crown and phosphate PCFs by varying ʌ and R_{eff}. Utilizing EIM technique, the analysis has been done in second and third telecom windows. With variation of the structural entities the modal parameter analysis has been monitored in the context of different material perspective that has remained as one of our chief objectives. Here, we have reckoned V parameter, Mode Field Diameter (MFD), beam divergence (θ) and Dispersion (D) that depict the modal properties of PCF.

Figures 2-4 illustrates the variation of the V parameter vs. λ in the range of O to L along with the additional fitting parameter Δn_d [5]. Hongbo Li et al., [5] have reported the fitting parameters n_{gc}, n_{cl}, n_g and Δn_d for solving the effective refractive index of PCF and by following the fitting parameters. Moreover, we build up our formulation in different material domain. With variation in effective core radii, diameter and pitches, the corresponding changes have been observed. The V parameter is found to be growing slowly for phosphate based PCF in each set of radii and it is found to fall under multi-mode region for radius 2ʌ-d with Δn_d = -7 x 10^{-4} and -15 x 10^{-4} [5]. On the contrary, crown PCF registers a characteristic fall under single-mode region, with a rapid variation within the considered range of wavelength. Besides, as shown in figures 2-4; increase in ʌ and R_{eff} brings the proposed PCF towards multi-mode region. This transition to multi-mode domain is realized by increase in number of modes which is caused by larger pitch values. Meanwhile, crown PCF, in this case, is found to follow single-mode operation in lower wavelength region in each set of pitch and effective core radii.

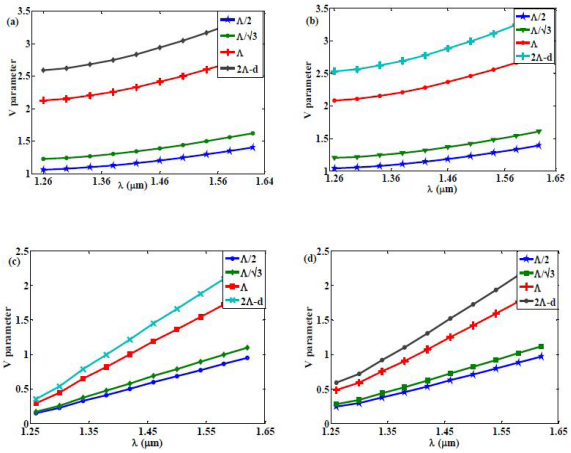

Figure 2: *V* vs. λ with *Λ*=2.3μm with (a) Δn_d=7 x 10^{-4} and (b) Δn_d=15 x 10^{-4} for phosphate based PCF (c) Δn_d=7 x $10^{-4}$and (d) Δn_d=15 x 10^{-4} for crown PCF.

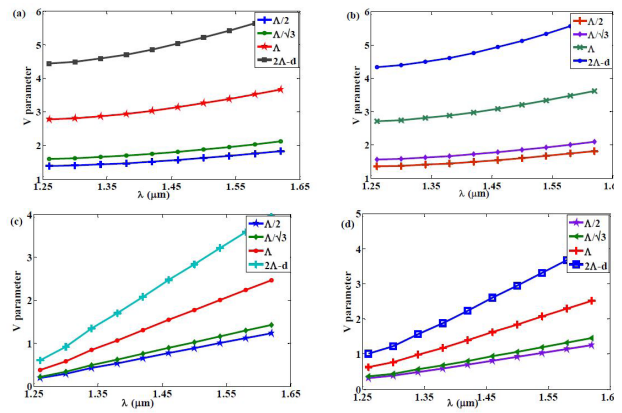

Figure 3: *V* vs. λ with Λ =3 μm with (a) Δn_d=7 x 10^{-4} and (b) Δn_d=15 x 10^{-4} for phosphate based PCF (c) Δn_d=7 x 10^{-4} and (d) Δn_d=15 x 10^{-4} for crown PCF.

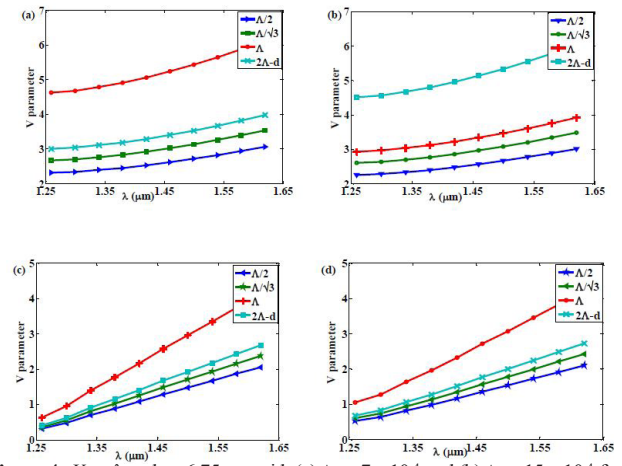

Figure 4: *V* vs. λ and Λ =6.75 μm with (a) Δn_d=7 x 10^{-4} and (b) Δn_d=15 x 10^{-4} for phosphate based PCF (c) Δn_d=7 x10^{-4} and (d) Δn_d=15 x 10^{-4} for crown PCF.

By inspecting the observable variation in V parameter with respective change in geometrical parameter the study has been extended to an important parameter for propagation i.e., mode filed diameter. Mode Filed Diameter (MFD) is considered as a crucial parameter for super continuum generation, soliton pulse transmission and optical signal processing [17-19]. The variation of MFD vs. λ in the considered band for each material PCFs has been illustrated in figures 5-7 respectively. The parameter is found to rise with increase in effective core radii and pitch. With increase in λ they show a rapid declining trend in case of crown PCF, whereas a moderate variation has been observed in phosphate PCF. During this study, it has been observed that MFD in both the PCFs decreases towards higher wavelength region. This trend can be utilized for a vast number of practical applications [10]. By considering the pattern of MFD vs. λ, it is evident that crown PCF exhibits an almost exponential decay pattern whereas phosphate PCF yields quite a steady linear decay instead. Higher values of refractive indices of cladding and core of crown PCF may be taken as one the plausible reason for this atypical decaying pattern of MFD vs. λ. In addition, it can be asserted that, with subsequent increase in pitch and core radii, the probability of the confinement of light towards the core decreases and that leads to diminution of MFD with respective change in wavelength band. The equation (1) shows that the V-parameter varies with n_{eff} which is a function of wavelength and the material index. Thus the V-parameter follows in figures 2-4 where it increases with wavelength for both phosphate and crown glass. In accordance with equation (2) it can be observed that spot size (w_{eff}) and correspondingly MFD (MFD=2w_{eff}) varies inversely to the V-parameter, thus with increase in wavelength as well as with V parameter the spot size decreases. For very small fiber cores with large Numerical Aperture (NA); the MFD is expected to increase with longer wavelengths in case of conventional fiber but in this case with introduction of materials of variable RI alters the effective refractive index and thus the changes can be observed. Since spot size varies with n_{eff} in PCF, thus the characteristic behavior of crown and phosphate PCF is observed in figure 5. This justifies our findings towards material aspects. Further, the relation between wavelength and refractive index for propagation of light also establishes our outcome. Besides, with increase in effective core radii (R_{eff}) and ∧ the parameter is found to increase in both the cases. One can also reckon this factor while going for fabrication and experimentations.

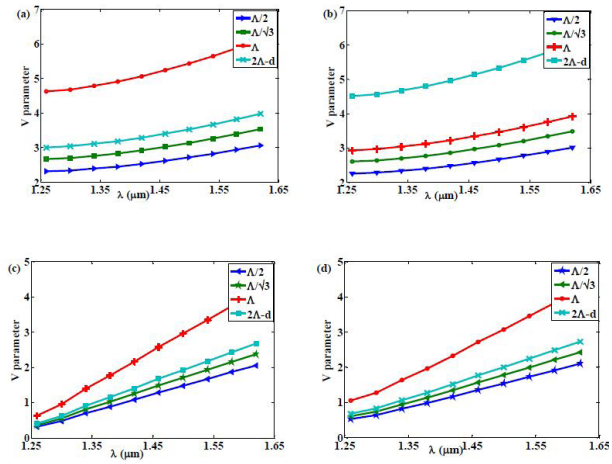

Figure 5: MFD vs. λ with Λ=2.3 μm with (a) Δn_d=7 x 10^{-4} and (b) Δn_d=15 x 10^{-4} for phosphate based PCF (c) Δn_d=7 x 10^{-4} and (d) Δn_d=15 x 10^{-4} for crown based PCF.

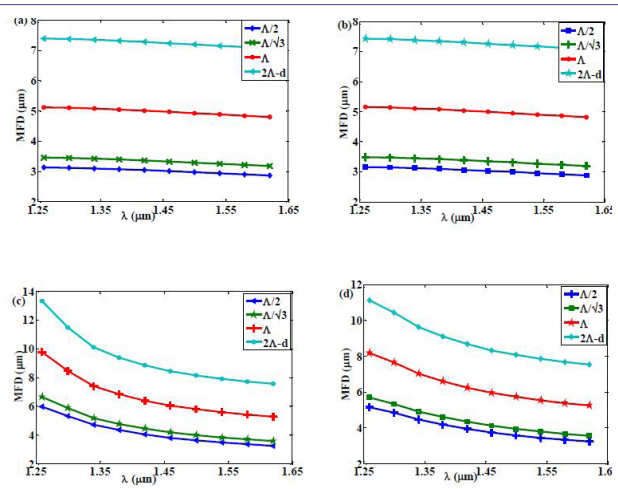

Figure 6: MFD vs. λ with Λ=3 μm with (a) Δn_d=7 x 10^{-4} and (b) Δn_d=15 x 10^{-4} for phosphate based PCF (c) Δn_d=7 x 10^{-4} and (d) Δn_d=15 x 10^{-4} for crown based PCF.

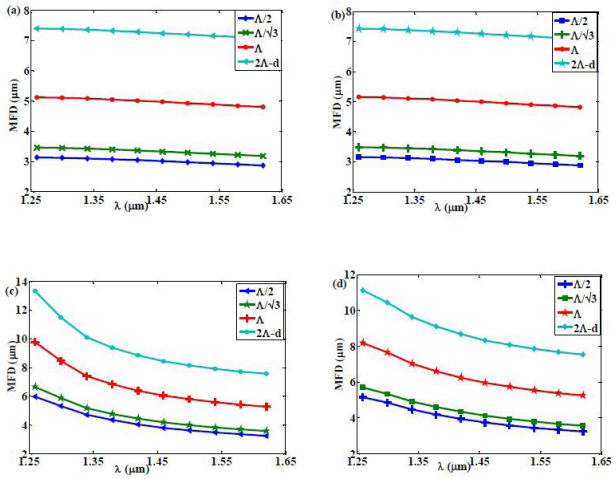

Figure 7: MFD vs. λ with Λ=6.75 μm with (a) Δn_d=7 x 10^{-4} and (b) Δn_d=15 x 10^{-4} for phosphate based PCF (c) Δn_d=7 x 10^{-4} and (d) Δn_d=15 x 10^{-4} for crown based PCF.

Further, the geometrical parameters have been incorporated to analyze beam divergence which is accountable to the quality control of the beam during propagation. In general, beam divergence in case of an electromagnetic beam implies the angular measurement of the radius with distance from the optical aperture as the beam propagates [9,10]. Figures 8-10 depict the corresponding plot of beam divergence vs. λ, entailing variable pitch and effective core radii. As evident in figures 8-10, beam divergence is found to increase with corresponding increase in λ. It is found to increase fairly for phosphate PCF and rapidly for crown PCF with respective change in geometrical parameters. Further, it is worthwhile to note that, with increase in pitch and core radii, the beam divergence is found to increase in each case. Crown PCF possesses lower values than that of phosphate based PCF.

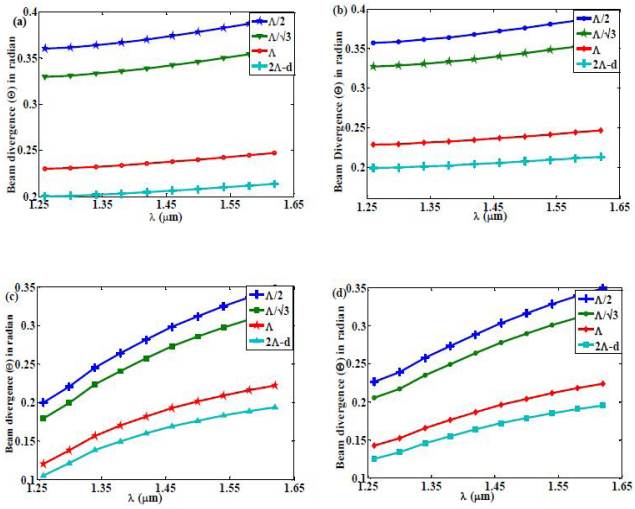

Figure 8: θ vs. λ with Λ=2.3 μm with (a) Δn_d=7 x 10^{-4} and (b) Δn_d=15 x 10^{-4} for phosphate based (c) Δn_d=7 x 10^{-4} and (d) Δn_d=15 x 10^{-4} for crown based PCF.

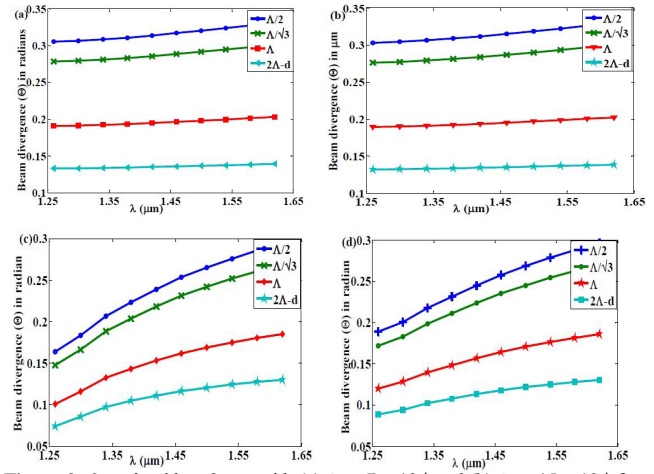

Figure 9: θ vs. λ with Λ=3 μm with (a) Δn_d=7 x 10^{-4} and (b) Δn_d=15 x 10^{-4} for phosphate based PCF (c) Δn_d=7 x 10^{-4} and (d) Δn_d=15 x 10^{-4} for crown based PCF.

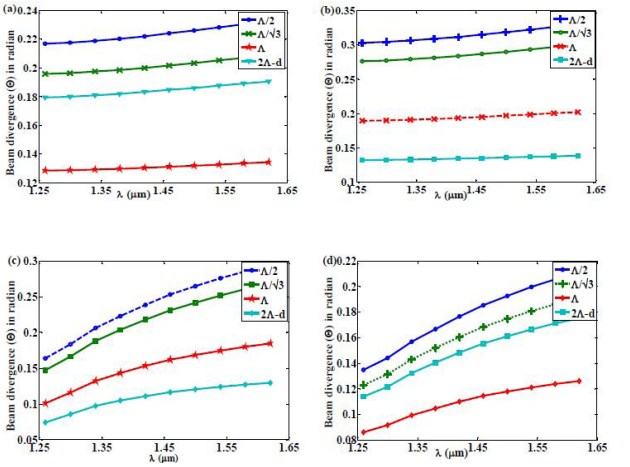

Figure 10: θ vs. λ with Λ=6.75 μm with (a) Δn_d=7 x 10^{-4} and (b) Δn_d=15 x 10^{-4} for phosphate based PCF (c) Δn_d=7 x 10^{-4} and (d) Δn_d=15 x 10^{-4} for crown based PCF.

In addition to the above parameters, the effective area (A_{eff}), as illustrated in figures 11-13, rises in accordance with larger pitch values and effective core radii. However, it registers a declining trend with increase in λ. And a moderate variation has been observed in case of phosphate based PCF whereas a rapid variation has been visible in crown based PCF. Moreover, in each set of PCF the observed values are found to increase with increase in pitch and effective core radii.

As the modal properties of PCF are also dependent upon dispersion. Thus, we assess dispersion for crown and phosphate PCF in the same structural domain. We have attained dispersion profile which is found to vary in large scale (Figure 14). As illustrated in figure 14(a), the variation of dispersion vs. λ has been considered in this context and it is seen that at higher wavelength region, dispersion estimates are considerably steady with respect to wavelength in phosphate PCF. However, crown PCF reveals negative dispersion. The dispersion provided in here depends upon the effective refractive index (n_{eff}) of the proposed photonic crystal fiber. Also, the change in material index

relates to n_{eff} of cladding which correspondingly alters dispersion. Since the dispersion depends upon RI and wavelength of propagation, thus introduction of variable RI can correspondingly change the dispersions in each case. The values of dispersion in case of phosphate and crown based PCFs are found to be ~7.43 x10^{-11} (0.0743 x10^{-9}) and -0.904x10^{-10} (0.0904 x10^{-8}) at 1.63 µm respectively over O to L communication band. So far, long-term communication is concerned, negative dispersion is very essential and crown PCF can be a better candidate for communication purposes. This validates our approach towards long-term communication purposes. As with increase in λ, the proposed PCFs can work under single-mode operation as well as it can be utilized for other practical applications. The overall changes in modal parameters that has been observed during this study have been enlisted in table 1.

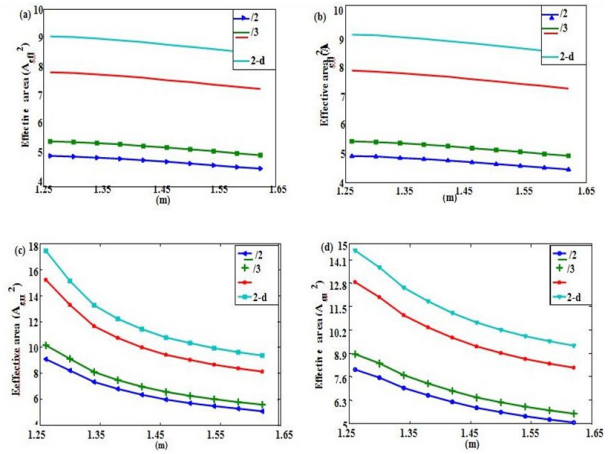

Figure 11: A_{eff} vs. λ with Λ=2.3 µm with (a) Δn_d=7 x 10^{-4} and (b) Δn_d=15 x 10^{-4} for phosphate based PCF (c) Δn_d=7 x 10^{-4} and (d) Δn_d=15 x 10^{-4} for crown based PCF.

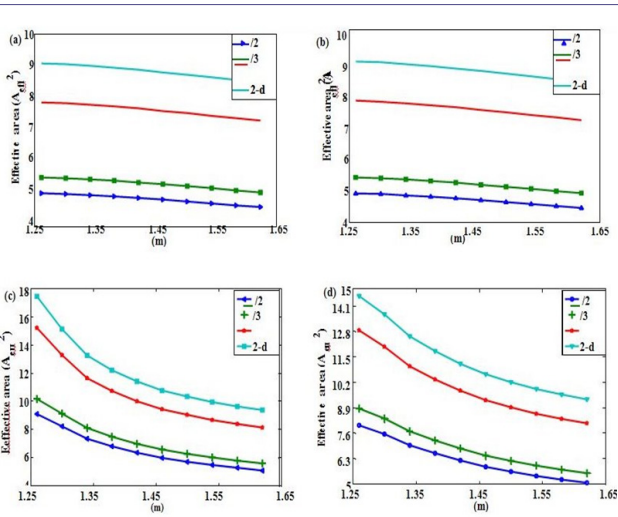

Figure 12: A_{eff} vs. λ with Λ=3 µm with (a) Δn_d=7 x 10^{-4} and (b) Δn_d=15 x 10^{-4} for phosphate based PCF (c) Δn_d=7 x 10^{-4} and (d) Δn_d=15 x 10^{-4} for crown based PCF.

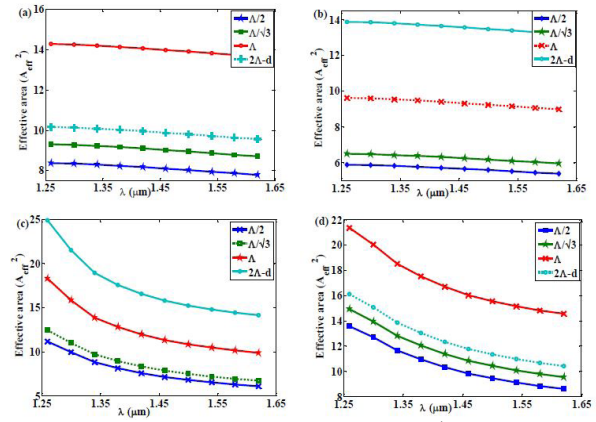

Figure 13: A_{eff} vs. λ with Λ=6.75 µm with (a) Δn_d=7 x 10^{-4} and (b) Δn_d=15 x 10^{-4} for phosphate based PCF (c) Δnd=7 x 10^{-4} and (d) Δn_d=15 x 10^{-4} for crown based PCF.

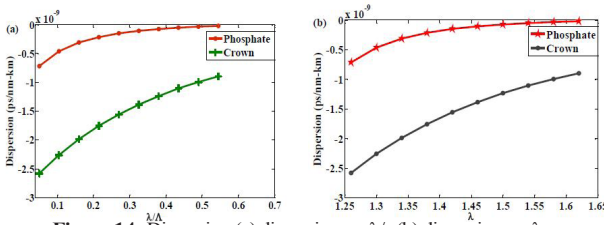

Figure 14: Dispersion (a) dispersion vs. λ/Λ (b) dispersion vs. λ.

Symbol	Quantity	Material Composition	Pitch	Overall Incremental Value	
				Δn_d= 7x10^{-4}	Δn_d= 15x10^{-4}
V	V parameter	Phosphate	2.3	1.53-2.02	Δn_d= 15x10^{-4}
			3	3.05-4.04	1.49-1.99
			6.75	0.69-0.918	2.98-3.98
		Crown	2.3	0.207-1.36	2.26-3.02
			3	0.413-2.71	0.348-1.39
			6.75	0.094-0.617	0.695-2.77
MED	Mode field diameter	Phosphate	2.3	2.16-2.24	0.158-0.629
			3	4.19-4.26	2.16-2.25
			6.75	0.963-0.947	4.195-4.27
			2.3	2.29-4.46	0.965-0.948
			3	4.31-7.36	2.28-3.54
		Crown	6.75	0.974-1.68	4.301-5.96
			2.3	0.16-0.18	0.972-1.36
θ	Beam divergence	Phosphate	3	0.173-0.192	0.159-0.177
			6.75	0.038-0.042	0.171-0.191
			2.3	0.095-0.153	0.171-0.191
			3	0.0898-0.164	0.101-0.154
		Crown	6.75	0.0898-0.165	0.101-0.166
			2.3	4.032-4.19	0.021-0.036
			3	7.84-7.97	4.039-4.21
A_{eff}	Effective area	Phosphate	6.75	1.77 - 1.799	7.84-7.99
			2.3	4.28 -8.339	7.841-7.986
			2.3	4.28 -8.339	4.267-6.624

Table 1: Estimated values of the phosphate and crown based PCF.

As reported elsewhere, the modal parameter analysis has been performed from L to C band i.e., 1.5-1.6μm and E to L band i.e., 1.36-1.63μm wavelength range in the context of two different materials [9,10]. The present work has focused on 2nd and 3rd communication window i.e., 1.23-1.63μm (O to L) λ range. The variation in V parameter in earlier study has been observed to be moderately rising in case of phosphate based PCF with lowest value ~2.59 in L to C and rapidly in case of crown based PCF with lowest value of ~1.58 in L to C for constant variation in parameter. And the lowest value of V was found to be ~2.52 and ~1.49 for phosphate PCF and crown based PCF respectively in E to L range. Similar kind of variation has been observed in present work too. But, in this study, the lowest value for phosphate and crown based PCF is found to be ~1.3 and 0.22 respectively for ʌ=2.3 μm. Besides, MFD of phosphate and crown based PCF is found to be ~2.8 μm and ~4.84 μm in E to L band and is found to be 2.82 μm ~ and ~5.12 μm in L to C band respectively. Whereas, in this present work for ʌ=2.3 μm, the values of MFD is found to be ~2.98μm and ~5.54μm for phosphate and crown based PCF. In L to C and E to L band the lowest value of effective area was found to be ~5.4μm^2 and ~ 5.3μm^2 for phosphate based PCF. And the values are found to be ~9.5μm^2 and ~9.2μm^2 for crown based PCF in L to C and E to L band respectively. In effective area (A_{eff}) variation with wavelength is found to decrease moderately in phosphate based PCF and rapidly in case of crown based PCF. The lowest value of phosphate and crown based PCF is found to be ~5.2μm^2 and 10.1μm^2 in O to L band at ʌ=2.3 μm. The beam divergence of phosphate and crown based PCF is found to be ~0.34 (rad) and ~0.2 (rad) in L to C band and is found to be ~0.336 (rad) and ~0.21 (rad) in E to L band respectively. Besides, variation in dispersion is found to vary rapidly in crown based PCF. Whereas, in earlier established results the dispersion variation is found to be moderate in both the cases. The overall change in modal parameter values are enlisted in table 2.

Symbol	Quantity	Pitch ((μM	Material Composition	Lowest Value of Each Parameter		
				$\Delta n_d = 7x10^{-4}$		
		2.3	Phosphate	L to C	E to L	O to L
V	V parameter			2.59	2.52	1.3
			Crown	1.58	1.49	0.22
MFD	Mode field (diameter (μm	-do-	Phosphate	2.82	2.8	2.98
			Crown	5.12	4.84	5.54
θ	Beam Divergence ((radian	-do-	Phosphate	0.34	0.336	0.345
			Crown	0.2	0.21	0.18
A_{eff}	Effective area ((μm^2		Phosphate	5.4	5.3	5.2
			Crown	9.5	9.2	10.1

Table 2: Comparative analysis study of previous work.

Noteworthy fact is that, the modal analysis performed for phosphate and crown based PCF follow the earlier trend as claimed in our previous work [9,10]. The previous works have been performed by encompassing constant pitch and effective core radii. However, a comprehensive study onto the modal parameter has been furnished in broader wavelength region and in variable geometrical parameters (ʌ, d and R_{eff}) domain in the context of phosphate and crown material. Also, it has been noticed that the parameters behave in accordance with our earlier published results [9,10] and further change in wavelength range has improved the quality of the proposed microstructured fiber. The attained results show that wavelength range has an impact onto the modal parameter. Further, it gives prominence to crown based PCF, which can be considered as a better candidate for future. In addition to that it has been observed that crown based PCF has more control over parameters than that of phosphate based PCF.

Conclusion

A comprehensive analysis of photonic crystal fiber has been accomplished utilizing Effective Index Method (EIM) in two material domains viz. phosphate and crown within a broad wavelength range (2nd and 3rd communication band). Throughout the study, three different air holes spacing (ʌ) and diameters (d) have been considered along with different effective core radii (R_{eff}). Based on these, all the computed parameters are studied, and a comparative analysis has been performed. As reported earlier in [9,10], it has been found that crown based PCF is preferable to that of phosphate based PCF which accommodate a higher mode field diameter and beam divergence which is indicative of low loss also. For, long haul communication purpose, both two materials based PCFs offer good standing while surpassing one another in some modal attributes. These results will prove beneficial for experimentalists to design PCFs for long distance communication purpose. Besides, the whole work covers the entire telecom window entailing all possible structural entities; hence, optical engineers can tailor their fibers according to their requirement based on the established results in this study and design them according to their requirement.

References

1. Knight JC (2003) Photonic crystal fibres. Nature 424: 847-851.
2. Saitoh K, Koshiba M (2005) Numerical Modeling of Photonic Crystal Fibers. J Lightwave Technol 23: 3580.
3. Limpert J, Liem A, Reich M, Schreiber T, Nolte S, et al. (2004) Low-nonlinearity single-transverse-mode ytterbium-doped photonic crystal fiber amplifier. Opt Express 12: 1313-1319.
4. Sharma DK, Sharma A (2012) On the mode field diameter of microstructured optical fibers. Opt Com 291: 162-168.
5. Li H, Mafi A, Schülzgen A, Li L, Temyanko VL, et al. (2007) Analysis and Design of Photonic Crystal Fibers Based on an Improved Effective-Index Method. J Lightwave Technol 25: 1224-1230.
6. Paschotta R (2010) Field Guide to Optical Fiber Technology. SPIE, Washington, USA.
7. Baggett JC, Monro TM, Furusawa K, Finazzi V, Richardson DJ (2003) Understanding bending losses in holey optical fibers. Opt Com 227: 317-335.
8. Wanga J, Jiang C, Hu W, Gao M (2006) Modified design of photonic crystal fibers with flattened dispersion. Opt Laser Technol 38: 169-172.
9. Paul D, Biswas R, Bhattacharyya NS (2015) Modal parameter analysis for crown glass and phosphate glass photonic crystal fiber. Indian J Phys 89: 737-741.
10. Paul D, Biswas R, Bhattacharyya NS (2015) Investigating photonic crystal fiber within E to L communication band with different material composites. Optik - International Journal for Light and Electron Optics 126: 4640-4645.
11. Knight JC, Birks TA, Russell PJ, Atkin DM (1996) All-silica single-mode optical fiber with photonic crystal cladding. Opt Lett 21: 1547-1549.

12. Birks TA, Knight JC, Russell PJ (1997) Endlessly single-mode photonic crystal fiber. Opt Lett 22**:** 961-963.

13. Ferrando A, Silvestre E, Miret JJ, Andre P, Andrés MV (2000) Vector description of higher-order modes in photonic crystal fibers. Journal of the Optical Society of America A 17: 1333-1340.

14. Knight JC, Arriaga J, Birks TA, Ortigosa-Blanch A, Wadsworth WJ, et al. (2000) Anomalous dispersion in photonic crystal fiber. IEEE Photonics Technology Letters 12: 807-809.

15. Li H, Mafi A, Schülzgen A, Li L, Temyanko VL, et al. (2007) Analysis and Design of Photonic Crystal Fibers Based on an Improved Effective-Index Method. J Lightwave Technol 25: 1224-1230.

16. Nielsen MD, Mortensen NA (2003) Photonic crystal fiber design based on the V-parameter. Opt Express 11: 2762-2768.

17. Chen M, Xie S (2008) New nonlinear and dispersion flattened photonic crystal fiber with low confinement loss. Opt Com 281: 2073-2076.

18. Ademgil H, Haxha S (2012) Endlessly single mode photonic crystal fiber with improved effective mode area. Opt Com 285: 1514-1518.

19. Saitoh K, Koshiba M (2005) Empirical relations for simple design of photonic crystal fibers. Opt Express 13: 267-274.

20. Miyagi K, Namihira Y, Razzak SMA, Kaijage SF, Begum F (2010) Measurements of mode field diameter and effective area of photonic crystal fibers by far-field scanning technique. Opt Review 17: 388-392.

21. Inci HD, Ozsoy S (2012) A theoretical study of large solid-core square-lattice silica photonic crystal fibers with square air-holes. Opt Materials 35: 205-210.

22. Koshiba M, Saitoh K (2003) Structural dependence of effective area and mode field diameter for holey fibers. Opt Express 11: 1746-1756.

23. Abdelaziz I, Ademgil H, AbdelMalek F, Haxha S, Gorman T, et al.(2010) Design of a Large Effective Mode Area Photonic Crystal Fiber with Modified Rings. Opt Com 283: 5218-5223.

24. Chand Er M, Sharma Er S, Sharma Er RK (2012) Demonstration of Chromatic Dispersion in Borosilicate Crown Glass Microstructure Optical Fiber. International Journal of Modern Engineering Research (IJMER) 2: 2591-2593.